Res Chem Intermed (2013) 39:569–583
DOI 10.1007/s11164-012-0580-3

Investigation of the reaction mechanism and kinetics of production of anhydrous sodium metaborate ($NaBO_2$) by a solid-state reaction

Mehmet Burçin Pişkin · Aysel Kantürk Figen · Hatice Ergüven

Received: 28 March 2012 / Accepted: 26 April 2012 / Published online: 15 May 2012

Abstract In this study, the solid-state reaction mechanism and kinetics were investigated for production of anhydrous sodium metaborate ($NaBO_2$), an industrially and technologically important boron compound. To assess the kinetics of solid-state production of $NaBO_2$, the chemical reaction between borax ($Na_2B_4O_7$) and sodium hydroxide (NaOH) was investigated by use of the thermal analysis techniques thermogravimetry (TG) and differential thermal analysis (DTA). DTA curves obtained under non-isothermal conditions at different heating rates (5, 10 and 20 °C/min), revealed five endothermic peaks corresponding to five solid-state reactions occurring at 70, 130, 295, 463, and 595 °C. The stages of the solid-state reaction used for production $NaBO_2$ were also analyzed by XRD, which showed that at 70 and 130 °C, $Na_2B_4O_7$ and NaOH particles contacted between the grains, and diffusion was initiated at the interface. However, there was not yet any observable formation of $NaBO_2$. Formation of $NaBO_2$ was initiated and sustained from 295 to 463 °C, and then completed at 595 °C; the product was anhydrous $NaBO_2$. Activation energies (E_a) of the solid-state reactions were calculated from the weight loss based on the Arrhenius model; it was found that in the initial stages of the solid-state reaction E_a values were lower than in the last three steps.

Keywords Sodium metaborate · Solid-state reaction · Arrhenius · Kinetics · Mechanism

M. B. Pişkin (✉)
Department of Bioengineering, Yıldız Technical University, Istanbul 34210, Turkey
e-mail: mpiskin@yildiz.edu.tr

A. K. Figen · H. Ergüven
Department of Chemical Engineering, Yıldız Technical University, Istanbul 34210, Turkey
e-mail: akanturk@yildiz.edu.tr

H. Ergüven
e-mail: haticeerguven@gmail.com

Introduction

Since 2005 Turkey has been the world's leading supplier of boron, with 72 % of the world's reserves and a market share of 37 %. The borates of sodium and their derivatives are the materials mostly used by the chemical and metallurgy industries. More than 230 boron derivatives are used in the production of >4,000 materials. Sodium metaborate compounds ($NaBO_2{\cdot}4H_2O$, $NaBO_2{\cdot}2H_2O$, $NaBO_2$), especially, are borax derivatives that can be used both as the powder or in solution for production of commercial boron compounds [1].

$NaBO_2$ is used in the chemical industry for production of photographic and textile chemicals, detergents, cleansers, and adhesives. It is also used for production of sodium perborate compounds ($NaBO_3{\cdot}nH_2O$) as the main material. $NaBO_2$ can also be incorporated in liquid laundry detergents for pH control, enzyme stabilization, and for its builder properties. Sodium metaborate tetrahydrate ($NaBO_2{\cdot}4H_2O$) is incorporated in many proprietary water-treatment chemicals requiring pH control and corrosion inhibition; these are used for protection against corrosion in central heating systems and cooling towers [2].

In recent years, because of the development and popularity of the use of hydrogen-powered energy, the demand for hydrogen storage with high energy density has increased. Hydrogen can be stored safely in boron minerals/compounds, for example as $NaBH_4$. $NaBH_4$, a known reducing agent, has been used as an anodic fuel in fuel cells or as a hydrogen-storage medium because of its high hydrogen-storage capacity (10.6 wt%). Use of anhydrous $NaBO_2$ in the energy industry, and the importance of commercial borates, are, therefore, gradually increasing [3–16].

Solid-state synthesis of boron compounds has been studied. Magnesium–boron compounds can be produced by solid-state reactions. $Mg_2B_2O_5$ and $Mg_3(BO_3)_2$ compounds are synthesized on the basis of solid-state principles [17]. The formation of boron nitride nanotubes by a solid-state process has also been investigated. Boron nitride nanotubes have been produced by annealing of ball-milled boron nitride powder in a nitrogen atmosphere. It has been shown that ball-milling is vital to formation of disordered boron nitride nanostructures, from which the nanotubes seem to grow by a solid-state process [18].

Generally, $NaBO_2$ is synthesized by a method from a mixture of borax and sodium hydroxide by the reaction shown in Eq. (1) [19]:

$$1/4\ Na_2B_4O_7 + 1/2\ NaOH + 5/4\ H_2O \rightarrow NaB(OH)_4{\cdot}2H_2O \quad (1)$$

When the reaction is complete, the saturated solution is filtered and cooled to room temperature, and crystals are formed. After synthesis, calcination must be performed to obtain anhydrous $NaBO_2$, in accordance with the equations:

$$NaB(OH)_4{\cdot}2H_2O \rightarrow NaB(OH)_4 + 2H_2O \quad (2)$$

$$NaB(OH)_4 \rightarrow NaBO_2 + 2H_2O \quad (3)$$

Investigation of the conditions for synthesis of anhydrous $NaBO_2$ from concentrated tincal ($NaBO_2{\cdot}10H_2O$) has previously been discussed in detail by our group. Anhydrous $NaBO_2$ was synthesized, in a single step, from concentrated

tincal. It was decided that concentrated tincal could be used as a starting material for production of anhydrous $NaBO_2$ without any purification procedure. The hydroxide phase is transformed into the hydrate structure by further heating, and the anhydrous form is obtained by heating at 400 °C for 5 h [20, 21].

Sodium metaborate tetrahydrate ($NaB(OH)_4{\cdot}2H_2O$) was also produced under the action of ultrasonic irradiation. It was shown that the reaction conditions (amount of water, temperature, and time) were of crucial importance in the synthesis of $NaB(OH)_4{\cdot}2H_2O$. The optimum conditions for the production process were 26 % water by weight, borax particles of size 250 ± 150 μm, and an irradiation time 60 min at 80 °C [22].

In this study, anhydrous $NaBO_2$ was produced on the basis of the principles of solid-state synthesis. The purpose of this study was to elucidate the reaction mechanism and the reaction kinetics for production of anhydrous $NaBO_2$ via a solid-state reaction. The chemical reaction between borax ($Na_2B_4O_7$) and sodium hydroxide (NaOH) was examined by use of thermal analysis (DTA, and TG) and X-ray diffraction analysis (XRD) to determine the reaction mechanism. Non-isothermal analysis was adopted to enable understanding of the reaction kinetics and activation energies (E_a), and the pre-exponential factors (k_0) were calculated by using the Arrhenius kinetic model. By observation of the crystalline phase and study of the kinetics, the optimum reaction conditions were determined and a solid-state reaction mechanism has been proposed.

Experimental

Materials and characterization

Anhydrous borax ($Na_2B_4O_7$) and sodium hydroxide (NaOH) were used as the starting materials in our experimental studies. $Na_2B_4O_7$ (ETIBOR-68) containing 68.00 % B_2O_3 and 30.27 % Na_2O was obtained from Bandirma Eti Mine Works, Turkey. Sodium hydroxide (NaOH, ≥95 % pure) was purchased from Merck.

The analyses performed for characterization in this study were:

(1) *DTA-TG analysis*: Thermal analysis of samples was performed by use of a Perkin Elmer Diamond TG\DTA instrument, which was calibrated by using the melting points of indium (T_m = 156.6 °C) and tin (T_m = 231.9 °C) under the same conditions as used for the sample. Samples were ground in an agate mortar and stored under an inert atmosphere before the analyses. Analyses were carried out at a heating rate of 10 °/min in an N_2 atmosphere at a constant flow rate of 100 ml/min. The samples were placed in standard Al_2O_3 crucibles and heated to 700 °C.

(2) *XRD analysis*: The crystalline structures of the solids were determined by XRD. X-ray analysis was conducted at ambient temperature by use of a Philips Panalytical X'Pert-Pro diffractometer with CuKα radiation (λ = 0.15418 nm) under operating conditions of 40 mA and 45 kV.

(3) *FT-IR analysis*: Attenuated total reflectance (ATR) FT-IR spectroscopy (Perkin Elmer Spectrum One) was used for identification of chemical bonds

of the samples. Before analysis, the crystal area was cleaned and the background was collected; the solid material was placed over the small crystal area on the universal diamond ATR top plate. The FT-IR spectrum was obtained after application of force to the sample, pushing it on to the diamond surface. The IR spectrum was recorded in the spectral range 4,000–650 cm^{-1}, at ambient temperature, and al a resolution of 4 cm^{-1}.

(4) *SEM analysis*: Scanning electron microscopy (Cam Scan) was used for identification of microstructures in the crystals. Before analysis the crystals were fixed to the sample plate with self-adhesive tape; they were then coated with gold for conductivity.

(5) *ICP–OES analysis*: Elemental analysis of the sample was performed by ICP–OES (Perkin Elmer, Optima 2100 DV). To prepare samples for analysis, the mineral was digested in hydrochloric acid–nitric acid–hydrofluoric acid–phosphoric acid (HCI–HNO_3–HF–H_3PO_4) solution. Samples were analyzed at least three times and mean values were used as a single observation.

Procedure and setup

Thermal analysis of the chemical reaction between borax ($Na_2B_4O_7$) and sodium hydroxide (NaOH) was performed to understand the solid-state mechanism of $NaBO_2$ production. A mixture of $Na_2B_4O_7$ and NaOH was prepared in a molar ratio of 1:2, in accordance with the $NaBO_2$ production reaction given in Eq. 4. The well-mixed powder was placed in the Al_2O_3-based high-temperature crucible of the TG/DTA instrument.

$$Na_2B_4O_7 + 2\ NaOH \rightarrow NaBO_2 \tag{4}$$

Differential thermal analysis (DTA) was performed from room temperature to 700 °C at different heating rates (5, 10 and 20 °C/min) to record any temperature difference between the sample and the reference. DTA is universally accepted by mineralogical laboratories as a rapid and convenient means of recording the thermal effects that occur as a sample is heated [23]. Temperature difference (ΔT) was plotted against temperature; the DTA curves obtained are given in Fig. 1. According to the results from non-isothermal DTA analysis, the solid-state reaction temperatures were 70, 130, 295, 463, and 595 °C, so solid-state reactions were performed at these specific temperatures for 5 h in a calibrated high-temperature furnace. The standard deviation of the internal temperature of the furnace was determined as ±1 °C. The crystalline phase and the chemical structure of the powders were examined by use of XRD to determine the optimum solid-state reaction temperature (Fig. 2). According to the crystalline phase results, the anhydrous $NaBO_2$ solid-state synthesis reaction occurred at 595 °C. FT-IR analysis were performed to characterize the molecular structure of the products; the FT-IR spectra obtained at different production temperatures are given in Fig. 3.

Kinetic analysis of the reaction for solid-state production of $NaBO_2$ was investigated on the basis of the Arrhenius kinetic model and Eqs. 5, 6, 7, and 8, below. Figure 4 shows the TG curve and the fractional conversion plots for the solid-state reactions. The order of the solid-state reaction was assumed to be unity ($n = 1$). According to the

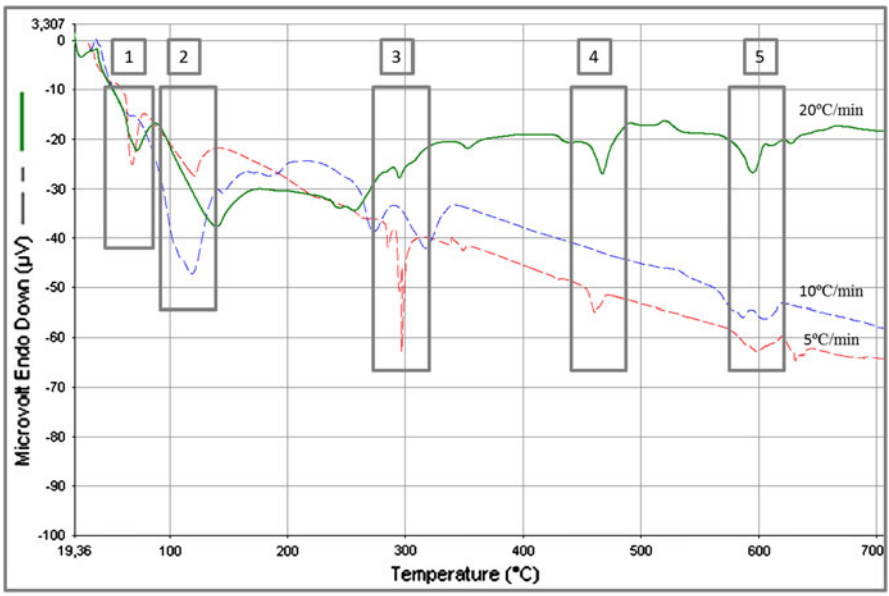

Fig. 1 Differential thermal analysis curves for the chemical reaction between $Na_2B_4O_7$ and NaOH

Arrhenius method, values of $\log\left[\left(\frac{dW}{dt}\right)\left(\frac{1}{W}\right)\right]$ were plotted against $1/T$ (Fig. 5). The equations for all the solid-state reactions are given in Table 1. The slopes of these lines, which were used to calculate E_a, were determined from the intercepts (Table 2).

$$\frac{dW}{dt} = k \times W^n \tag{5}$$

$$k = A_{r.} \exp\left(\frac{-E}{R.T}\right) \tag{6}$$

$$\frac{dW}{dt} = A_{r.} \exp\left(\frac{-E}{R.T}\right) \times W \tag{7}$$

$$\log\left[\left(\frac{dW}{dt}\right) \times \left(\frac{1}{W}\right)\right] = \log A_r - \frac{E}{2.303.R.T} \tag{8}$$

Elemental analysis, microstructural analysis, and bulk density measurements were also conducted to identify all the properties of the final product synthesized under optimum reaction conditions (595 °C and 5 h). ICP–OES results and SEM images are given in Table 3 and Fig. 6, respectively.

Results and discussion

Anhydrous sodium metaborate ($NaBO_2$) production by solid-state reaction

The reaction powder obtained from mixing of the starting materials ($Na_2B_4O_7$ and NaOH), was heated from the room temperature to 700 °C at heating rates of 5, 10

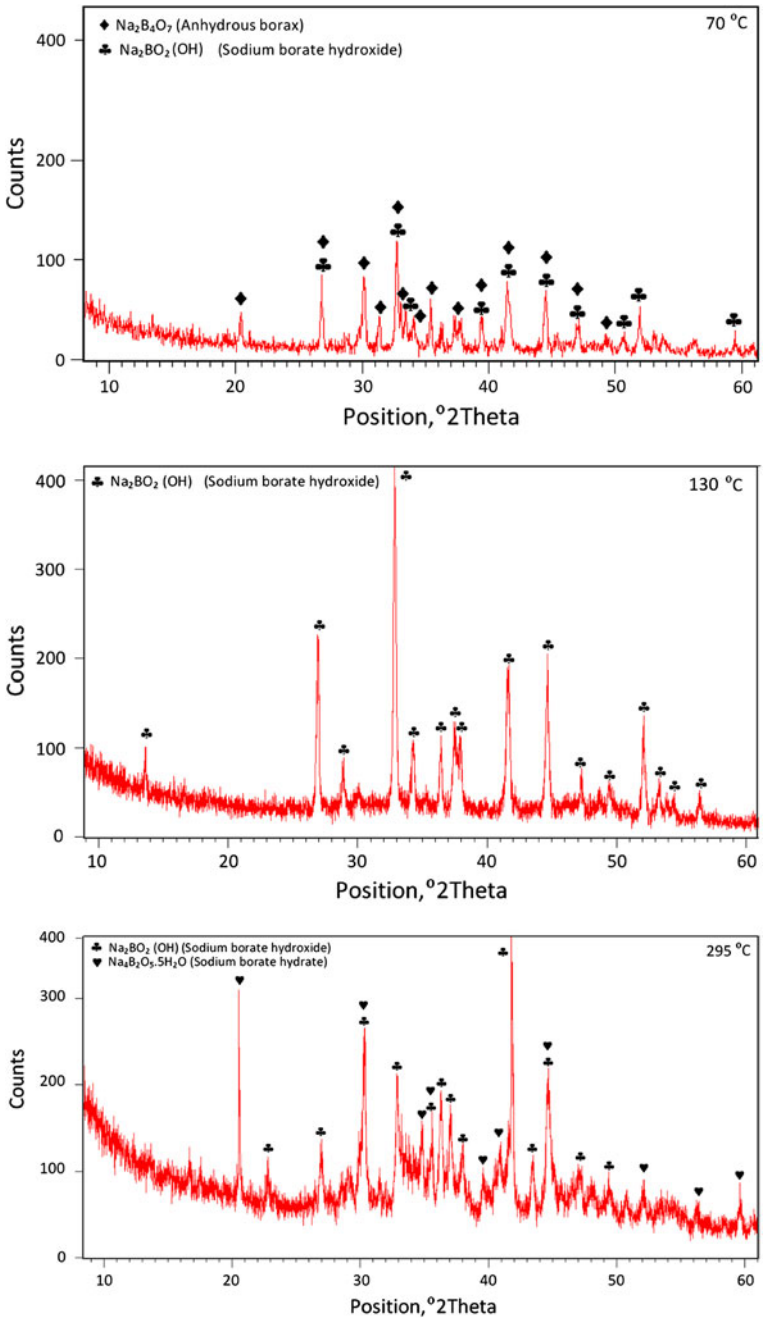

Fig. 2 XRD patterns of powders synthesized at different temperatures

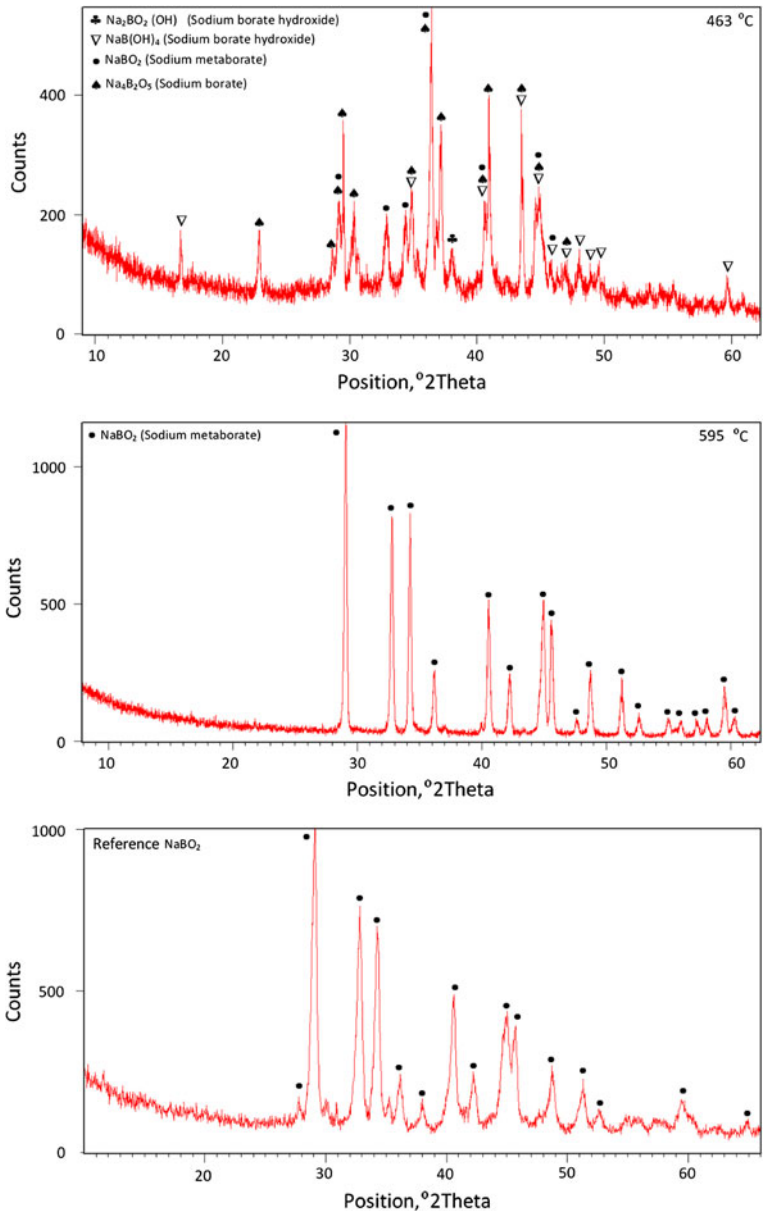

Fig. 2 continued

and 20 °C/min. The corresponding DTA curves are illustrated in Fig. 1. As indicated by the DTA curves, five endothermic peaks were observed; these peaks corresponded to different solid-state reactions. Taking into consideration each heating rate, the profiles of the DTA curves were indicative of similar behavior, and

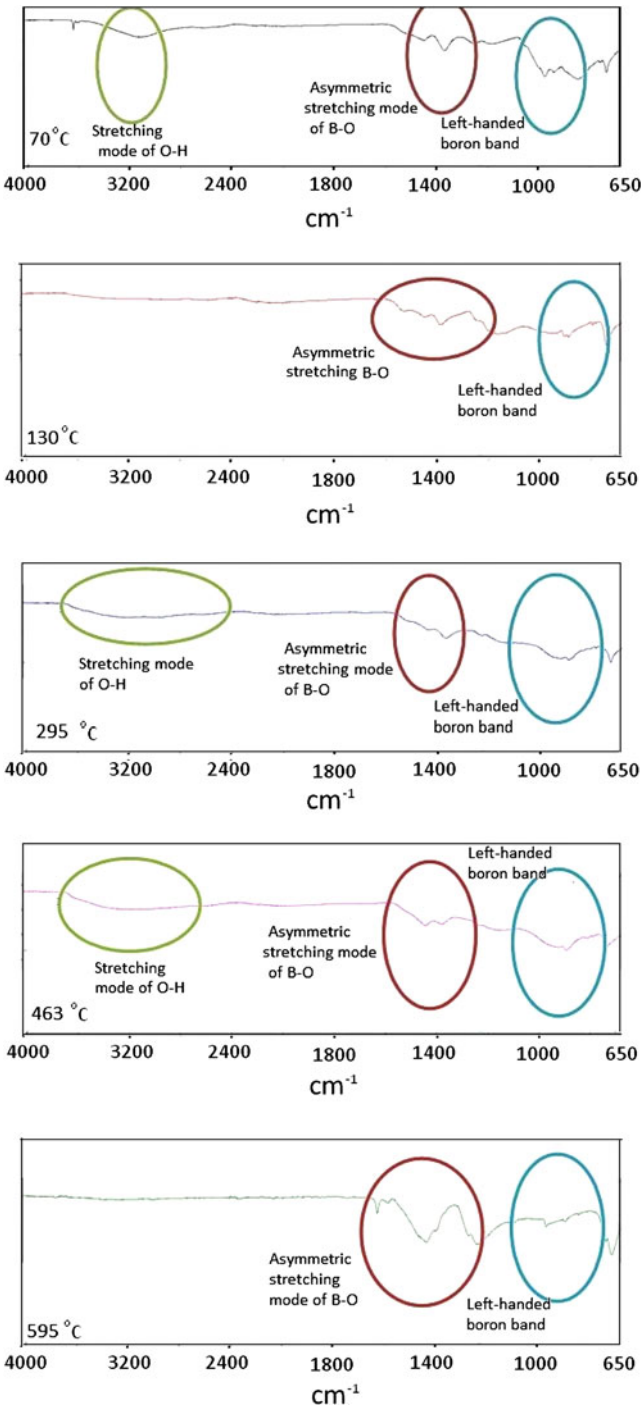

Fig. 3 FT-IR spectra of powders synthesized at different temperatures

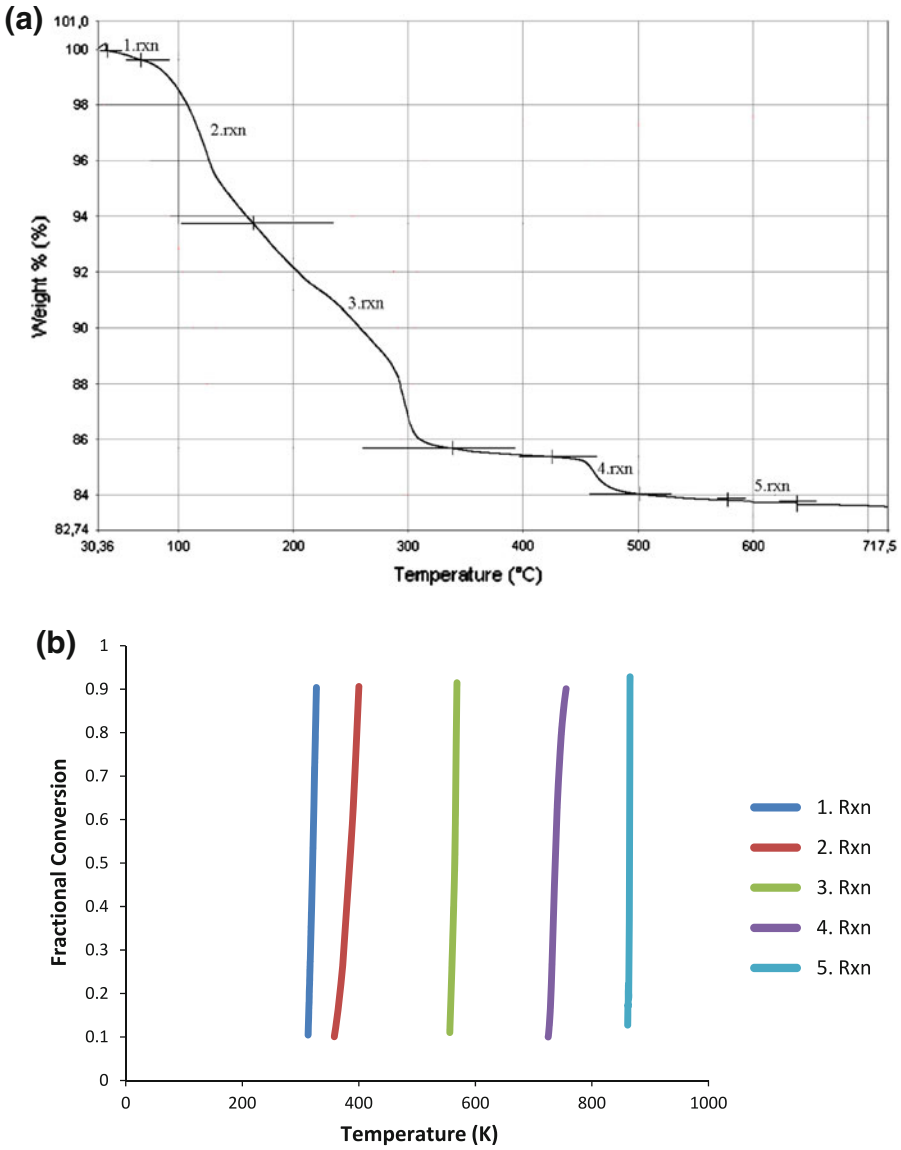

Fig. 4 Thermogravimetric curve (**a**) and fractional conversion plots (**b**) for the solid-state reactions

the maximum peak temperatures (T_m) of the DTA curves were noted, to define the solid-state reaction temperatures. The assumption that the T_m occurs when the reaction rate is maximum was supported by the experimental work. It was observed there was no significant difference in the maximum peak temperature (T_m) of the DTA curves. It is, therefore, best to use the average maximum peak temperature (ΣT_m) for the solid-state synthesis reactions. The ΣT_m of solid-state reactions were

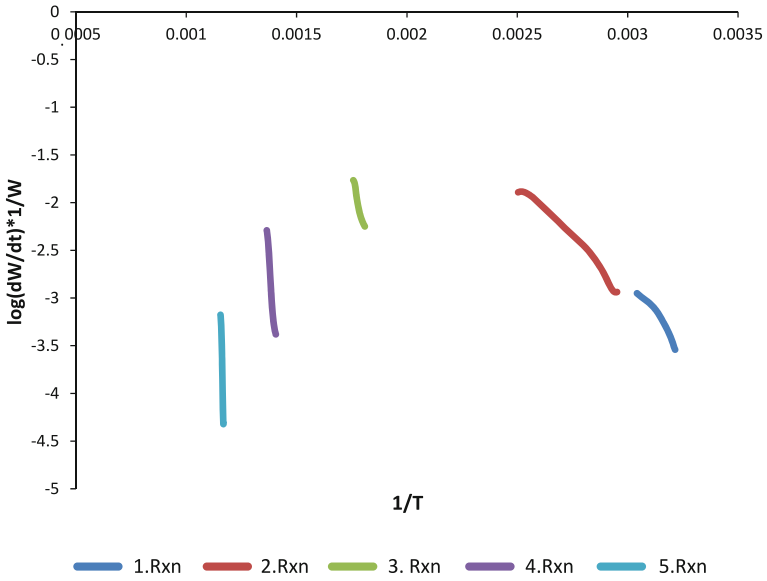

Fig. 5 Arrhenius kinetic model plots for the solid-state reactions

Table 1 Arrhenius model kinetic equations for the solid-state reactions

Reactions	Equations	R^2
1	$y = -3458x + 7.64$	0.9559
2	$y = -2293x + 3.91$	0.9717
3	$y = -10622x + 16.90$	0.9704
4	$y = -30601x + 39.482$	0.9774
5	$y = -100479x + 113.06$	0.9703

Table 2 Activation energies (E_a) of the solid-state reactions

Reaction	E_a (kJ/mol)
1	66.21
2	43.90
3	203.38
4	585.92
5	1923.88

calculated as 70, 130, 295, 463, and 595 °C. At these five temperatures, the reaction powder was heated for 5 h to determine the reaction mechanism.

The stages of the solid-state reactions were analyzed by XRD. The XRD pattern of $NaBO_2$ standard is given, as a reference, below the other XRD patterns in Fig. 2, to enable comparison of the results from the analysis with those of the product, $NaBO_2$. $NaBO_2$ standard was prepared as indicated in our previous study [20].

Table 3 ICP–OES elemental analysis results for the final product

Element	Concentration (ppm)
S	745.43
Ca	140.85
Fe	15.425
Si	>0.5
As	>0.02

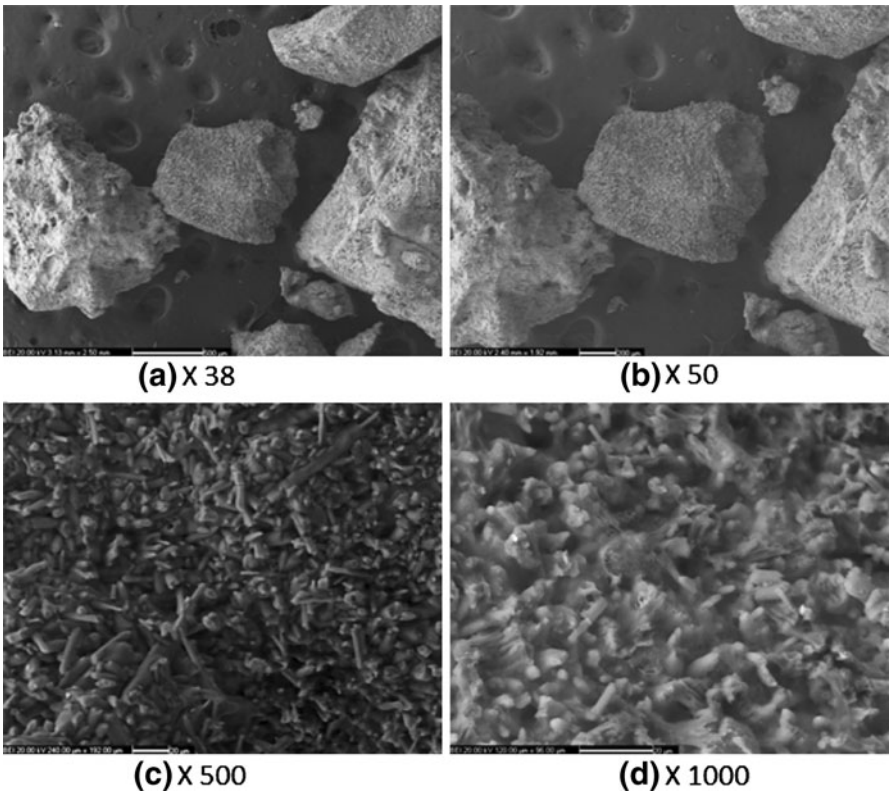

Fig. 6 SEM images of the final product

As indicated by the XRD results, formation of $NaBO_2$ was accompanied by an increase in the solid-state synthesis temperature. At low temperatures, the main phase was the hydroxide structure and $NaBO_2$ did not form. Further heating of the mixture caused the hydroxide phase to be converted into the hydrate phase as the reaction temperature was increased to 463 °C, and the sodium metaborate structure began to form. As can be seen from the XRD pattern of the sample synthesized at 595 °C, all the peaks detected were associated with the anhydrous $NaBO_2$ structure; the sodium boron hydroxide and sodium borate hydride phases were no longer

present. It was determined that the solid-state synthesis temperature required to produce $NaBO_2$ was 595 °C.

Figure 3 shows the FT-IR spectra of the products obtained at 70, 130, 295, 463, and 595 °C. The FT-IR analysis showed the stretching mode of O–H at the beginning of the reaction, but this disappeared as the temperature increased. The bands at 1,573 and 1,571 cm^{-1} were assigned to the bending mode of H–O–H. The bands at 1,436 and 1,422 cm^{-1} were assigned to asymmetric and symmetric stretching, respectively, of B–O.

Kinetic investigation of the solid-state reaction

Figure 4a shows the TG curve obtained during heating of the powder obtained by mixing of the starting materials ($Na_2B_4O_7$ and NaOH). In addition, the fractional conversion values were plotted against reaction temperature for the five basic solid-state reactions; these are shown in Fig. 4b.

Five stages of mass loss corresponding to the five solid-state reactions were apparent from the TG curve, as was also apparent from the DTA curves. In the first two steps the total weight loss was 0.341 and 5.898 % in the temperature ranges 38.01–72.71 and 72.71–156.08 °C, respectively. In the third, fourth, and fifth steps, corresponding to the temperature ranges 275.55–338.65, 425.16–501.54, and 582.71–603.88 °C, respectively, the weight losses were 8.094, 1.338, and 0.081 %.

Non-isothermal kinetic calculations were performed for all the steps on the basis of the Arrhenius equation, assuming a first-order reaction. Values of $\log\left[\left(\frac{dW}{dt}\right)\left(\frac{1}{W}\right)\right]$ were plotted against $1/T$ (Fig. 5) and the kinetic plots (Table 1) were used to calculate the kinetic data (Table 2). For the initial stages of the solid-state reaction (first and second steps), E_a values were lower than for the last three steps. In the last two steps, E_a values increased because of the formation of $NaBO_2$, and even more energy was required to produce anhydrous $NaBO_2$.

At 70 and 130 °C, $Na_2B_4O_7$ and NaOH particles contacted between the grains, and then diffusion was initiated at the interface. However, there was not yet any observable formation of $NaBO_2$. Formation of $NaBO_2$ was initiated and sustained from 295 to 463 °C, and then completed at 595 °C, with formation of anhydrous $NaBO_2$.

Mechanism of $NaBO_2$ production by solid-state reaction, and structural observations

Structural characterization of the final product, and confirmation of its synthesis under the optimum conditions (595 °C, 5 h) were achieved by use of XRD, FT-IR, SEM, ICP–OES, and the bulk density test (TS 2573).

The microstructure of the final product; $NaBO_2$ was investigated by SEM analysis, the results for which are shown in Fig. 6. According to the SEM images, the particles were similar to each other and were distributed homogeneously; average particle size was calculated as approximately 630.56 μm.

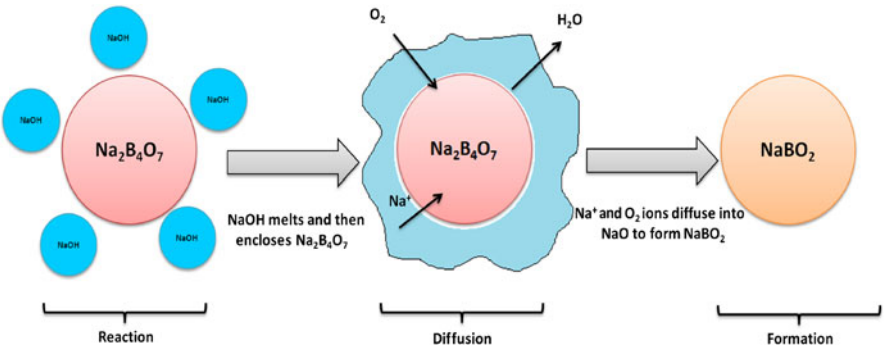

Fig. 7 Mechanism of formation of anhydrous $NaBO_2$ by the solid-state reaction

ICP–OES was used to determine five elements (S, Ca, Fe, Si, and As) in the final product, $NaBO_2$. The results are summarized in Table 3. It can be seen that all these elements were present in trace amounts, originating from the main raw material.

Bulk density measurements were performed as stated in the Turkish Standard 2573 [24]. Bulk density is defined as the mass of many particles of the material divided by the total volume they occupy. Bulk density is an important property of solid products taken into account in the packaging of the commercial product [25]. The final product was analyzed at least three times and the mean values were used as a single observation. The bulk density of the final product, $NaBO_2$, was calculated as 1.0249 g/cm^3. For this reason, the bulk density of $NaBO_2$ could be reported as "freely settled" and there was no need for a specified compaction process during packaging.

In view of these analytical results, a solid-state reaction mechanism was proposed; this is illustrated in Fig. 7. As the synthetic temperature increased, $Na_2B_4O_7$ at the surface reacted with NaOH forming a shell of $NaBO_2$ accompanied by release of H_2O. Because of melting of the NaOH, the $Na_2B_4O_7$ was enclosed. With increasing synthesis time, the reactive NaOH diffused into the core of the $Na_2B_4O_7$, thickening the $NaBO_2$ shell. The diffusion process was completed by exhaustion of the raw materials, eventually forming the pure anhydrous $NaBO_2$ phase.

Conclusion

In this study, the mechanism of synthesis of anhydrous $NaBO_2$ from $Na_2B_4O_7$ was investigated in detail. Anhydrous $NaBO_2$ is an industrially and technologically important boron compound, specifically used in $NaBH_4$ production. If anhydrous $NaBO_2$ could be synthesized more economically, storage of hydrogen as $NaBH_4$ could be more applicable.

The following points result from this study:

(1) A general procedure based on a solid-state reaction mechanism was developed for synthesis of anhydrous $NaBO_2$. Anhydrous $NaBO_2$ was synthesized from $Na_2B_4O_7$ in a one-step, solid-state reaction.
(2) The hydroxide phase was transformed into the hydrate structure by heating, then the anhydrous form was obtained. The reaction was studied by use of analytical methods, and the optimum reaction conditions were found to be reaction at 595 °C for 5 h.
(3) As indicated by kinetic investigation of the solid-state reaction, synthesis of $NaBO_2$ occurred in five reaction steps. In the initial stage of the solid-state reaction the E_a values were lower than those in the last steps. E_a values increased with increasing temperature.
(4) Synthesis of anhydrous $NaBO_2$ from $Na_2B_4O_7$ was initiated on the surface by melting of NaOH, which enclosed the $Na_2B_4O_7$. With increasing calcination temperature reactive NaOH diffused into the core of $Na_2B_4O_7$ thickening the $NaBO_2$ shell.

References

1. The Report of Chemical Industry, Turkey State Planning Organization, 2001
2. E.D. Garret, *Borates, Handbook of Deposits, Processing, Properties and Use, vol. 401* (Elsevier, San Diego, 1998)
3. Y. Kojima, T. ve Haga, Recycling process of sodium metaborate to sodium borohydride. Int. J. Hydrogen Energy **28**, 989–993 (2003)
4. Z.P. Li, B.H. Liu, N. Arai, S. ve Suda, Protide compounds in hydrogen storage systems. J. Alloy. Compd. **356–357**, 469–474 (2003)
5. U.B. Demirci, P. ve Miele, Sodium tetrahydroborate as energy/hydrogen carrier, its history. C. R. Chimie **12**, 943–950 (2009)
6. Z.P. Li, B.H. Liu, J.K. Zhu, N. Morigasaki, S. ve Suda, $NaBH_4$ formation mechanism by reaction of sodium borate with Mg and H_2. J. Alloy. Compd. **437**, 311–316 (2007)
7. B.H. Liu, N. Morigasaki, S. Suda, Kinetics characteristics of sodium borohydride formation when sodium meta-borate reacts with magnesium and hydrogen. Int. J. Hydrogen Energy **33**, 1323–1328 (2008)
8. H.B. Liu, Z.P. Li, J.K. ve Zhu, Sodium borohydride formation when mg reacts with hydrous sodium borates under hydrogen. J. Alloy. Compd. **476**, L19–L20 (2009)
9. H. Zhang, S. Zheng, F. Fand, G. Chen, G. Sang, D. ve Sun, Synthesis of $NaBH_4$ based on a solid-state reaction under Ar atmosphere. J. Alloy. Compd. **484**, 352–355 (2009)
10. T. Kemmitt, G.J. ve Gainsford, Regeneration of sodium borohydride from sodium metaborate and isolation of intermediate compounds. Int. J. Hydrogen Energy **34**, 5726–5731 (2009)
11. USP 2.534.533. Methods of Preparing Alkali Metal Borohydrides, United State Patent (1950)
12. H.I. Schlesinger, H.C. Ve Brown, Uranium (IV) borohydride. J. Am. Chem. Soc. **75**, 219–221 (1953)
13. H.I. Schlesinger, H.C. ve Brown, Metallo borohydrides. Lithium borohydride. J. Am. Chem. Soc **62**, 3429–3435 (1940)
14. H.I. Schlesinger, R.T. Sanderson, A.B. ve Burg, Metallo borohydrides. I. Aluminum borohydride. J. Am. Chem. Soc. **62**, 3421–3425 (1940)
15. H.I. Schlesinger, H.C. Brown, H.R. Hoekstra, L.R. ve Rapp, Reactions of diborane with alkali metal hydrides and their addition compounds. New syntheses of borohydrides. sodium and potassium borohydrides. J. Am. Chem. Soc. **75**, 199–204 (1953)
16. H.I. Schlesinger, H.C. Brown, A.E. ve Finholt, The preparation of sodium borohydride by the high temperature reaction of sodium hydride with borate esters. J. Am. Chem. Soc. **75**, 205–209 (1953)

17. H. Güler, F. Kurtuluş, E. Ay, G. Çelik, I. Doğan. Solid-state and microwave-assisted synthesis and characterization of $Mg_2B_2O_5$ and $Mg_3(BO_3)_2$, processing of 4. international boron symposium Eskişehir, (2009), 129–137
18. Y. Chen, L.T. Chadderton, J.F. Gerald, J.S. Williams, A solid-state process for formation of boron nitride nanotubes. Appl. Phys. Lett. **74**, 20 (1999)
19. A. Kanturk, M. Sari, S. Piskin, Synthesis, crystal structure and dehydration kinetics of $NaB(OH)_4 \cdot 2H_2O$. Korean J. Chem. Eng. **25**, 1331 (2008)
20. A. Kanturk, S. Piskin, Parametric investigation on anhydrous sodium metaborate ($NaBO_2$) synthesis from concentrated tincal. Adv. Powder Technol **21**, 513–520 (2010)
21. A. Kanturk, H. Erguven, S. Piskin, in *Investigation of solid state reaction mechanism for sodium metaborate ($NaBO_2$) production*. Supplemental Proceedings: MaterialsProcessing and Energy Materials, vol 1 (2011), pp. 585–589. doi:10.1002/9781118062111.ch67
22. S.M. Yılmaz, K.A. Figen, S. Pişkin, Production of sodium metaborate tetrahydrate ($NaB(OH)_4 \cdot 2H_2O$) using ultrasonic irradiation P. Powder Technol. **215–216**, 166–173 (2012)
23. H.E. Kissinger, Variation of peak temperature with heating rate in differential thermal analysis. J. Res. Natl. Bur. Stand. **57**(4), 217–221 (1956)
24. TSE 273, Sodium perborates for industrial use determination of bulk density, (ISO 3424) (1975)
25. O. Buckman Harry, C. Brady Nyle, *The Nature and Property of Soils—A College Text of Edaphology*, 6th ed. (MacMillan Publishers, New York, 1960)